Geodesy and Geodynamics 9 (2018) 50–56

Contents lists available at ScienceDirect

Geodesy and Geodynamics

journal homepages: www.keaipublishing.com/en/journals/geog; http://www.jgg09.com/jweb_ddcl_en/EN/volumn/home.shtml

Goce derived geoid changes before the Pisagua 2014 earthquake

Orlando Álvarez [a, b, *], Mario Gimenez [a, b], Andrés Folguera [d], Sofia Guillen [c], Claudia Tocho [c]

[a] Instituto Geofísico y Sismológico Ing. Volponi, FCEFyN, Universidad Nacional de San Juan, Argentina
[b] Consejo Nacional de Investigaciones Científicas y Técnicas, Argentina
[c] INDEAN – Instituto de Estudios Andinos "Don Pablo Groeber", Departamento de Cs. Geológicas, FCEN, Universidad de Buenos Aires, Argentina
[d] Facultad de Ciencias Astronómicas y Geofísicas, Universidad Nacional de La Plata, Argentina

A R T I C L E I N F O

Article history:
Received 21 April 2017
Accepted 18 September 2017
Available online 13 December 2017

Keywords:
Satellite gravimetry
Pre-seismic geoid changes
Great megathrust earthquakes
Subduction zones
Forecasting and monitoring

A B S T R A C T

The analysis of space – time surface deformation during earthquakes reveals the variable state of stress that occurs at deep crustal levels, and this information can be used to better understand the seismic cycle. Understanding the possible mechanisms that produce earthquake precursors is a key issue for earthquake prediction. In the last years, modern geodesy can map the degree of seismic coupling during the interseismic period, as well as the coseismic and postseismic slip for great earthquakes along subduction zones. Earthquakes usually occur due to mass transfer and consequent gravity variations, where these changes have been monitored for intraplate earthquakes by means of terrestrial gravity measurements. When stresses and correspondent rupture areas are large, affecting hundreds of thousands of square kilometres (as occurs in some segments along plate interface zones), satellite gravimetry data become relevant. This is due to the higher spatial resolution of this type of data when compared to terrestrial data, and also due to their homogeneous precision and availability across the whole Earth. Satellite gravity missions as GOCE can map the Earth gravity field with unprecedented precision and resolution. We mapped geoid changes from two GOCE satellite models obtained by the direct approach, which combines data from other gravity missions as GRACE and LAGEOS regarding their best characteristics. The results show that the geoid height diminished from a year to five months before the main seismic event in the region where maximum slip occurred after the Pisagua $Mw = 8.2$ great megathrust earthquake. This diminution is interpreted as accelerated inland-directed interseismic mass transfer before the earthquake, coinciding with the intermediate degree of seismic coupling reported in the region. We highlight the advantage of satellite data for modelling surficial deformation related to pre-seismic displacements. This deformation, combined to geodetical and seismological data, could be useful for delimiting and monitoring areas of higher seismic hazard potential.

1. Introduction

The convergence of the Nazca and South American Plates (65 mm/y rate and N75°E azimuth [1]) explains long-term deformational patterns along the Peru–Chile margin. The western edge of South America undergoes partly elastic deformation during the interseismic period [2]. Gradual accumulation of crustal deformation (mainly fore- and intra-arc shortening) occurs during the interseismic stage, considering seismic cycle deformation as explained within the framework of the purely elastic rebound theory [3]. The study of the deformational field over seismic regions (e.g. interplate) is a key issue for understanding the mechanical

* Corresponding author. Ruta 12 Km 17, Jardín de los Poetas, Rivadavia, San Juan, Argentina.
E-mail addresses: orlando_a_p@yahoo.com.ar, orlando.alvarez@conicet.gov.ar (O. Álvarez).
Peer review under responsibility of Institute of Seismology, China Earthquake Administration.

Production and Hosting by Elsevier on behalf of KeAi

https://doi.org/10.1016/j.geog.2017.09.005

processes that occur during crustal strain accumulation and sudden relaxation from inter-to co-seismic stages along the seismic cycle.

Determination of surficial displacements at regional scale in subduction zones requires quantification of centimetre displacements over large areas, the ocean and high mountainous areas. During the interseismic period, the interplate contact remains coupled and blocked, accumulating strain and elastic energy between plates along the subduction zone. As the interplate contact continues locked, converging plates are brittle-ductile and also elastically deformed (prior to the main shock) driving tectonic uplift of the upper plate in the forearc region. Prior to rupture, a period of accelerated deformation develops, in which precursor signals may occur (e.g. absence or increase of seismicity, variations of seismic wave propagation parameters, fluid chemical composition and pressure, electrical resistivity, radon levels, etc. [4]. Additionally, gradual crustal uplift or subsidence, depending on the observation point location with respect to the epicentre and the mechanism of the future earthquake, are among long-term precursors. During the interseismic period the upper plate undergoes ductile deformation in the lower part and brittle deformation in the upper part. Furthermore, it has been observed in the north-central Chilean margin that shallow crustal seismicity in the upper plate of the marine forearc is characterized by contractional shallow events [5].

Modern geodesy as Global Positioning System (GPS), Synthetic Aperture Radar interferometry (InSAR)and satellite gravimetry (GRACE, GOCE), allows to precisely quantify surface displacements associated with both interseismic strain build up and coseismic strain release along plate boundaries [6]. Modelling deformation at a regional scale facilitates the characterization of the short-term seismic cycle behaviour and its relation to the long-term tectonic evolution [7]. Models based on geodetical data (GPS, InSar) allowed determining slip models, stress and strain behaviour, seismic coupling degree, convergence rate, etc. [6,8–12]. On the other hand, gravity field variations allowed inferring mass transfer before and after earthquake occurrence [13–18]. Geoid changes are useful for quantifying crustal deformation that could be related to tectonic mechanisms as well as deeper causes as viscoelastic behaviour of the mantle.

In this work, we used the gravity signal from GOCE (Gravity Field and Steady State Ocean Circulation Explorer) satellite in order to model preseismic deformation along plate interface expressed by means of geoid heights variations. GOCE models from Ref. [19] GO_CONS_GCF_2_DIR_R4 (Nov. 1, 2009–Aug. 1, 2012) and GO_CONS_GCF_2_DIR_R5 (Nov. 1, 2009–Oct. 20, 2013) cover a data span between Aug. 2012 and Oct. 2013 allowing to model gravity variations prior to the Pisagua $Mw = 8.2$ great megathrust earthquake on April 24 2014, the greatest earthquake after GOCE mission ending.

2. Gravity variations and earthquake monitoring

Gravity variations are presently considered of great importance for understanding the development and occurrence of earthquakes [20]. Terrestrial gravity variations provide information about crustal mass transfer [21,22] and have proved to be useful in predicting occurrence and particularly locations of medium to large intraplate earthquakes [20,23,24]. These regional gravity anomaly variations and high gravity gradients along the related active faults before earthquakes can be used as seismic precursors. Local positive gravity variations near the epicentre and occurrence of high-gravity-gradient zones across the epicentre prior to intraplate earthquakes were reported in several cases [20,25].

Different studies have shown the usefulness of gravity satellite derived data for studying both coseismic and postseismic deformation, and consequent gravity changes from major earthquakes [13–16,26–29]. These results, based on satellite gravity data, are consistent with other geodetic measurements [30]. The long wavelength characteristic of satellite derived gravity field models allows comparison and analysis of the rupture zones of great megathrust earthquakes that occur along the plate interfaces. In these regions, where subducting and upper plates are in a close contact, after slip and viscoelastic relaxation involve the lower crust and upper mantle.

Earthquake interseismic and postseismic deformations influence broad areas including the offshore, where terrestrial gravity measurements are scarce and their changes is difficult to be monitored. In these regions, the distribution of satellite derived gravity anomalies and gravity gradients present a close relation to rupture zones [31–33]. Recent works focused on the Peruvian-Chilean convergent margin [17,18] have shown gravity variations after the Maule and before the Iquique-Pisagua earthquakes based on GOCE TIM models. Similarly, Fuchs, M.J. et al. [16] found that gravity changes detected by GOCE gradient trends were related to coseismic slip for the Tohoku earthquake, through analysing GOCE gravity gradiometry raw data.

3. Data and method

GOCE models present homogeneous data quality (precision) as no terrestrial data enter into their computation, avoiding consequent induced errors or sampling biases typical of terrestrial gravity measurements. One of the main problems of terrestrial data is the non-uniformity of the database (different campaigns) and lack of coverage in regions with difficult access (high mountains) or no availability (offshore). This is well solved by satellite missions as satellite data present homogeneous precision and quality, although with lower spatial resolution than achieved by terrestrial data or combined models as EGM2008 [34] (a spatially heterogeneous combination of data). Even though satellite models only provide information on the long wavelength part of the spectrum [35], spatial resolution is not a major problem when analysing great megathrust rupture zones, since involved areas are in the range of hundreds of km^2 according to the last GOCE derived models. Half wavelength spatial resolutions ranging from 60 to 80 km are achieved with the GO_CONS_GCF_2_TIM_R4/R5 [36]and the GO_CONS_GCF_2_DIR_R4/R5 [19,37] satellite GOCE models. The smallest resolvable feature of the gravity field or spatial resolution is given by $\lambda/2 = \pi R/N$, where R is the Earth radius and N is the degree/order of the model [38].

The geoid is expressed as a first approximation by Bruns' formula [39]:

$$N\,(\lambda,\phi) = \;T\,(0,\lambda,\phi)/\gamma(0,\phi) \tag{1}$$

It is obtained from the anomalous potential (T) regarding the normal gravity (γ) (see Ref. [38] for a detailed explanation). It can be directly calculated from the Earth gravity field model expressed as a series of spherical harmonic coefficients [38,40].

Geoid is representative of a hypothetical equipotential surface of the Earth following the mean level of the oceans at rest that is prolonged under the continents. Geoid changes show a variation of this equipotential surface and are related either to exogenous forces (topographic erosion) or to endogenic forces (mass redistributions inside the Earth interior). However, large variations on one-year time-scale mainly represent the crustal response to accelerated mass redistributions inside the Earth.

In the present work, we calculated geoid heights from the GOCE models GO_CONS_GCF_2_DIR_R4 and R5 [19,37]. These models are based on the direct approach combining kinematic GOCE orbit data, GOCE gradiometer data, and data from LAGEOS and GRACE (measurement period of ten years: 2003–2012). The model GO_CONS_GCF_2_DIR_R4 (developed up to $N = 260$) has an effective data volume of ~837 days (~13,430 orbital revolutions) covering a span from Nov. 1, 2009 to Aug. 1, 2012. The model GO_CONS_GCF_2_DIR_R5 (developed up to $N = 300$) has an effective data volume of ~1259 days (~19,380 orbital revolutions) covering a span from Nov. 1, 2009 to Dec. 20, 2013. We calculated the difference between both models up to the same degree/order of 260, obtaining geoid changes between Aug. 1, 2012 and Oct. 20, 2013. In GO_CONS_GCF_2_DIR_R5 datasheet, the main characteristics of the model are shown in comparison to the previous releases of the GOCE direct approach. The spectral behaviour of DIR-R5 presents a formal error (expressed in terms of geoid height) significantly smaller compared to that of DIR-R4, being the difference in terms of geoid heights of 0.002 m for $N = 260$ (see Fig. 1 of datasheet_go_cons_gcf_2_dir_r5). The cumulated geoid error at 100 km resolution is estimated at 1.7 cm for DIR_R5 model [37], being the cumulated formal error equal to 0.8 cm at degree/order 200.

4. Results and discussion

On April 1, 2014, a $Mw = 8.1$ megathrust earthquake occurred offshore Northern Chile, south of the Arica bend (Fig. 1), at the location of (70.769°W, 19.610°S)and at a depth of 25 km (USGS catalogue). A strong aftershock with $Mw = 7.6$ followed the main shock on April 3, 2014 at approximately 110 km to the Southeast. The main rupture propagated more than 150 km along the margin and the maximum slip reached up to approximately 5 m [41–45].

Before the Iquique-Pisagua sequence in 2014, the northern Chile margin presented a well-identified seismic gap since the rupture of 1877 (~137 years ago). The 2014 earthquake broke a highly coupled segment (Fig. 1) of this gap [12,43,46,47]. Increased seismic rates were reported in the months prior to the 2014 rupture, with peak magnitudes during the last three weeks before the main shock [43,48]. Specifically, more than 1300 events with magnitude above Mw 3.0 occurred during the 15 months preceding the main shock, so this event had an extensive preparation phase [48]. In fact, the seismic activity had steadily increased since 2008 with repeated interplate thrust events of $Mw < 4.0$, revealing global catalogues an increase in seismicity in the region since 2005, compared with the previous 10 years [43].

The Peru–Chile margin is mainly erosive at these latitudes with a high plate coupling and increased shear stresses where the trench is almost starved of sediments (up to 500 m) [49–52]. Leon-Rios et al. [53] proposed that the spatial distribution of re-located foreshocks and aftershocks, and its seismological characteristics was strongly controlled by the rheological and tectonic conditions of the extreme erosive margin of Northern Chile.

Ruiz et al. [43] found that the inference of a low coupling zone (Fig. 1) off the coast of Iquique implies some degree of accommodation of plate convergence by aseismic slip, which might operate by repeated slow slip events (SSE) (either the magnitude of these SSEs was too small, or they occurred too far from the coast to be detected by GPS measurements). Their results suggest

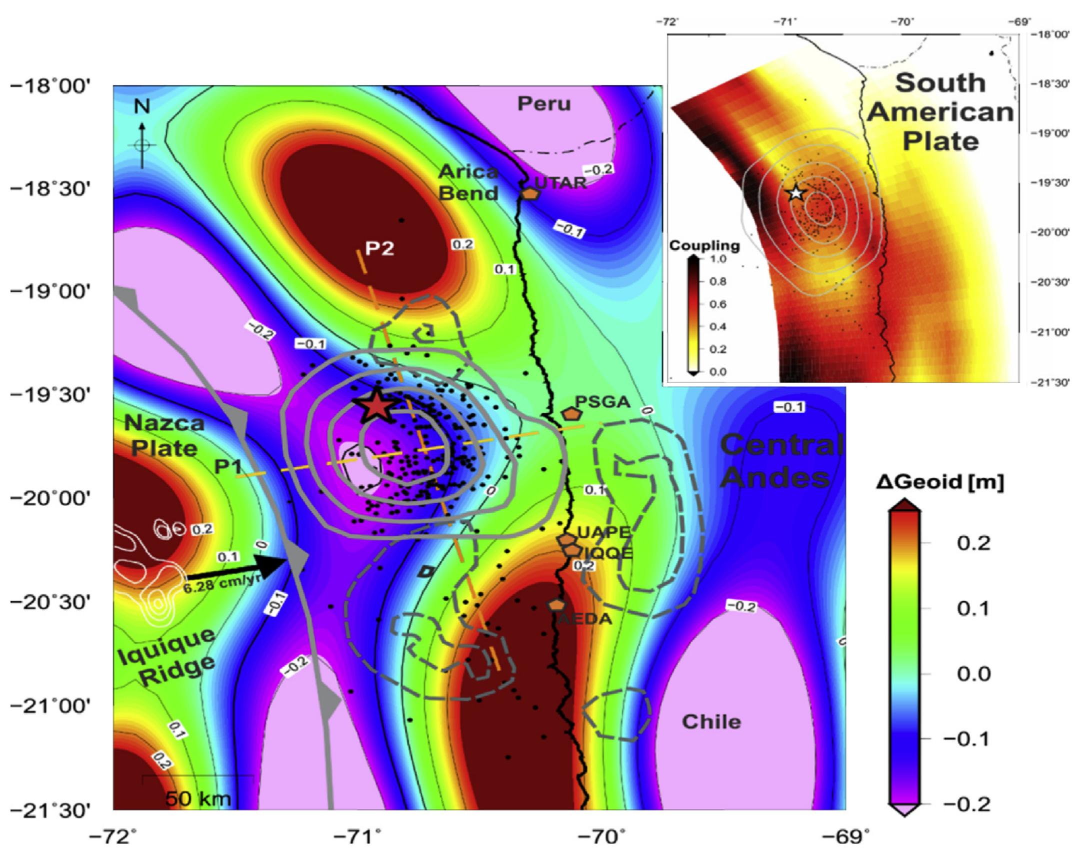

Fig. 1. Geoid height(s) variations (colour contours) from 1.5 to 0.5 year before the Pisagua-Iquique sequence. Maximum slip of 4 m (grey solid 1 m-contour line, [45] on April 1, 2014 is centered in the region of maximum geoid diminution. Here, a lobe of −0.2 m in geoid changes coincides in geometry with the maximum slip lobe six months prior to earthquake occurrence. Dashed grey contours depict the foreslip model from Ref. [45]. In the right upper corner the interseismic locking degree from Ref. [12] is plotted, where a value of 1 corresponds to full locking while 0 corresponds to creeping at the long-term plate convergence. Here, two relative minima can be observed to the north and south of the main rupture [42]. Then, the main rupture occurred on a region with intermediate locking degree, and an interseismic inland-directed ground displacement could be inferred by means of geoid diminution.

that interseismic loading has been decreasing in the Iquique area during the past decade, probably reflecting a very SSE occurring on the decadal time scale.

More recently, Socquet, A. [45] found that long-term aseismic slip of the subduction interface led to the nucleation of the $Mw = 8.1$ Pisagua-Iquique megathrust earthquake. This long-term precursory phase based on geodetic precursor (GPS) occurred simultaneously with an identified increase in the seismicity rate and decrease in b-value [42]. The preseismic displacement within 8 months (from July 2013 to mid-March 2014) suggests that a slow slip event (corresponding to a $Mw = 6.5$ earthquake, 80% of which was aseismic in nature) occurred on the subduction interface surrounding the main shock slip patch (Fig. 1). Analysing the accelerating seismic activity in the time frame of months to days prior to large earthquakes at plate interfaces in the North Pacific, Bouchon M. [54] suggested that at plate boundaries, the interface between the two plates begins to slowly slip before the interface ruptures during a large earthquake.

Large geoid variations outside the rupture area, to the north and south respectively, are presented as paired negative-positive geoid anomalies at the marine forearc (Fig. 1). Trenchwards, the geoid diminution is dominated by the subduction of the Nazca plate, in this region both plates are highly coupled (close to 1, [12]) and subduction erosion produces a collapse of the trench slope [55,56].

The positive geoid change to the coastline (to the north and south of the rupture) indicates that the overriding South American plates lowly slips in a zone of low coupling during the interseismic period [12].

In the region of maximum slip of the main shock on April 1st, geoid heights decreased continuously along the entire outer forearc (Figs. 2 and 3) for at least 5–6 months before the earthquake. Such change in the geoid signal could be dominated by margin subsidence in a region where higher locking degree was reported [12] and no foreslip occurred up to March 16, 2014 [45].

Ruiz et al. (2014, supplementary material Fig. S11) [43] plotted the position of stations located along the coast in the period from January 2013.0 to 2014.4 (after subtraction of the interseismic and seasonal terms, and removal of outliers after estimation of both white and flicker noise). Close GPS stations (PSGA, UAPE and IQQE) showed a rate increase in the eastward movement from July 2013 to approximately October 2013, namely in the last 3–4 months of GOCE mission. However, distant stations (UTAR and AEDA) didn't show such variation in coincidence to this anomalous behaviour of the central part (See Fig. 1 for stations location).

Geoid height variations prior to the Iquique-Pisagua earthquake showed a decrease of 10–20 cm coinciding with the posterior maximum slip of this region (Figs. 2 and 3) between one year and six months before event occurrence. Geoid height variations show a minimum lobe of 20 cm to the west-southwest (opposite to the convergence direction) of the main slip, with similar shape and geometry to the maximum slip lobe (Fig. 1).

This decrease in geoid height could be interpreted as the long-term gravitational collapse (due to margin subsidence) of a segment of the outermost forearc (as explained by Refs. [55,56] by means of gravity falls), which was locked to the down-going plate during the interseismic period (Fig. 2). Part of this geoid diminution

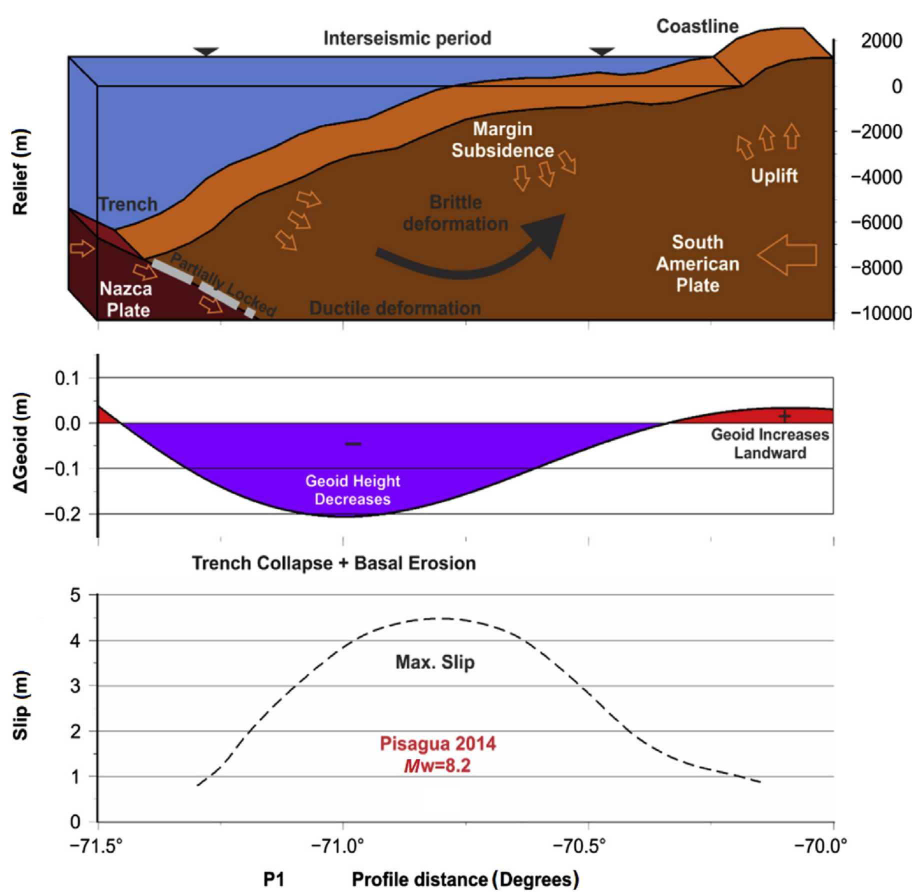

Fig. 2. Trench perpendicular profile (P1 in Fig. 1) following convergence direction. During the interseismicphase the plate interface remains locked at different degrees producing brittle-ductile deformation on the upper plate. Deformation is detected at these stages by geoid height changes obtained from satellite GOCE mission, constituting a potential forecasting tool. Evidence of brittle deformation occurred in the upper part of the overriding plate is provided by inversed events during the interseismic period [5]. Ductile deformation occurs in the lower part of the upper plate where quartz-rich rocks present low resistance to the deformation at high temperatures [57].

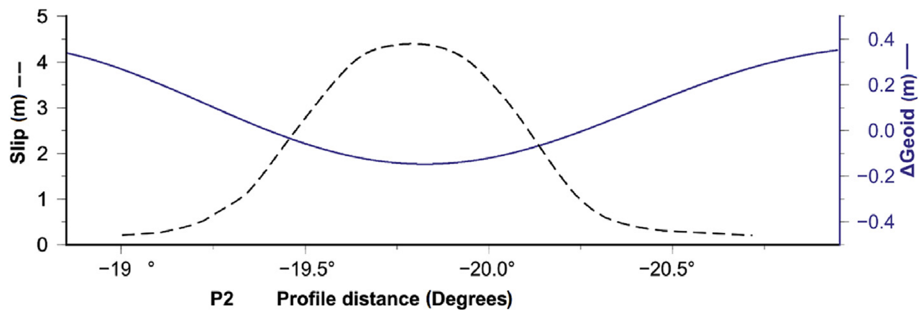

Fig. 3. Trench parallel profile across maximum slip (P2 in Fig. 1). Maximum slip coincides latitudinally with geoid height diminution prior to Pisagua $Mw = 8.2$ earthquake. Geoid changes from satellite gravimetry could serve for delimiting regions with higher seismic hazard along the interplate.

could be the expression of brittle-ductile deformation during the interseismic period and an increase of hydro fracturing. Wells et al. (2003) [32] found a link between slip, subsidence, and subduction erosion in basin-centered asperities in great subduction zone earthquakes by means of gravity anomalies. Thus, a plausible mechanism for such a geoid diminution could be localized subsidence, in which the geoid minimum indicates the region with higher (differential) deformation along the margin. Then maximum slip during main rupture (and foreslip from 15 days before; see Ref. [45] coincided with the area of continuous geoid decrease along the marine forearc.

The existence of three latitudinal segments (Fig. 4) with different coupling degrees, could explain that the central region, where geoid diminished continuously, differentially stored higher elastic energy at least 5–6 months before the main shock. This energy began to release in the region of the main rupture as slow slip [41,45], with intense foreshock activity at least three months before the main shock [43,48].

At the Nazca plate, between 20°S and 20.5°S, the northern expression of the Iquique ridge constitutes a prominent high oceanic feature (white contour in Fig. 1), which coincides with a positive change in geoid heights. This relation could be explained as

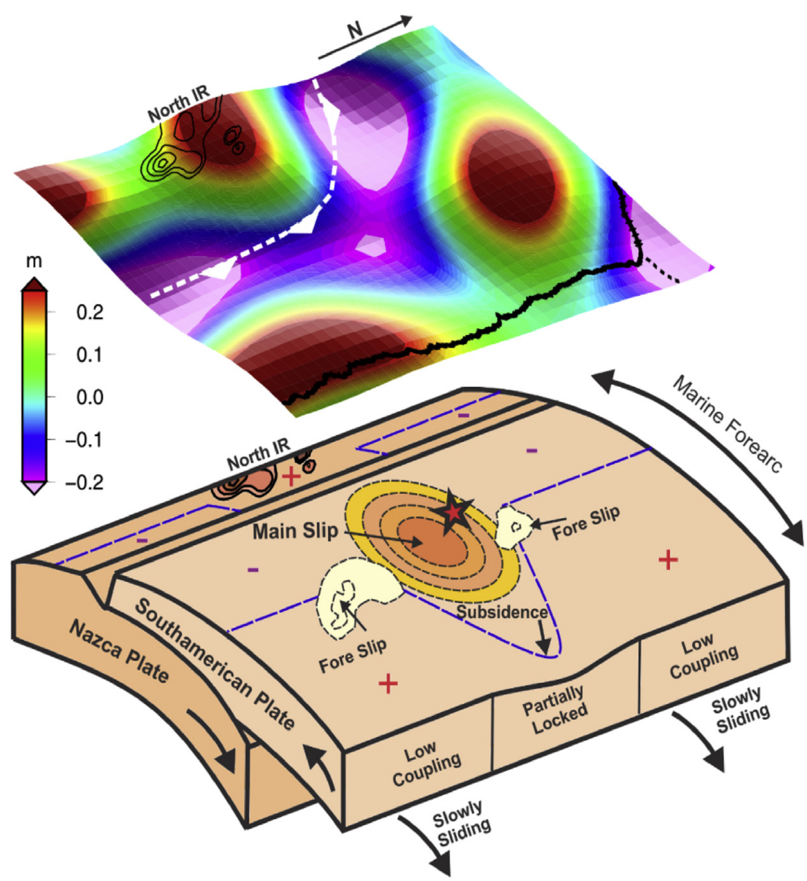

Fig. 4. Schematic interpretation of Geoid changes between Aug. 1, 2012 and Oct. 20, 2013 from GOCE. Geoid diminution along the trench and along the central segment are related to regions of higher seismic coupling degree (see Fig. 1). This gravitational collapse is interpreted as dominated by the effect of margin subsidence and trench collapse due to subduction erosion. Regions along the marine forearc where geoid height increased, are interpreted as the combined effect of aseismic slip and foreslip in zones where coupling is low and plates are slowly sliding. The central region began to seismically release the stored elastic energy three months before (foreshock sequence), increasing this foreshock activity 15 days up to the main shock and slowly slipping this segment. Then on April 1st, 2014, after the main shock occurred, the plate interface ruptured with an area similar to geoid height diminution (central lobe).

the differential uplift of sea floor surrounding due to a higher buoyancy of the oceanic crust prior to subduction. Subducted aseismic ridges can influence seismicity and plate-interface coupling, explaining nets of small earthquakes and rupture ends of large earthquakes [55]. Subduction of these bathymetric highs could produce higher basal erosion, upper plate faulting, creeping (long foreshock sequences), changes in coupling along their flanks [55]and margin subsidence along the entire forearc with consequent long-term gravitational collapse along the central segment.

The geoid diminution along the continental forearc could be composed by two main components, one related to upper crust elastic rebound (extension and subsidence during interseismic period) and another associated with the isostatic effect of the subducting slab (dynamic topography).

The surficial velocity field obtained from an extensive array of GPS (more than 10 years of measurements in northern Chile) plus InSar data, provided a detailed picture of the variable interseismic coupling (ISC, ratio of the slip deficit rate and the long-term slip rate) on the megathrust interface [2,6,12]. The rate of moment deficit over the 1877 rupture segment was of approximately 16.5×10^{21} Nm after the Tocopilla earthquake which corresponds to the energy released by an earthquake of moment magnitude $M\text{w} = 8.8$ over the whole 1877 rupture area, as reported by Chlieh, M. [6]. More recently, Metois, M. [12] identified along-strike variations in the average interseismic coupling from GPS velocity inversion (Fig. 1). Different interseismic coupling models [2,6,12] show a higher coupling where maximum slip took place, while the last two ISC models are consistent with the obtained geoid changes.

Large geoid variations in just one year of measurements could represent not only the result of a relatively sudden movement between the two coupled plates (as indicated by foreslip models), but also to a long term physical change at the plate interface as indicated by ISC [12] and the start of the decrease in b value, 3 years before the main shock [42].

5. Conclusions

Satellite gravimetry proved in the last years to be an important quantity to study crustal mass heterogeneities and its relation to earthquakes and seismic cycle. Changes in the Earth gravity field, expressed as geoid height variations, caused either by mass transfer, tectonic deformation or by the viscoelastic behaviour of the mantle throughout a portion of the interseismic cycle, seem to be a good precursor signal to determine future rupture dimensions. Regions of high interseismic coupling mapped from other geodetical methods (GPS and InSar) are expected to coincide with large seismic slip, although the breaking of these locked fault zones is difficult to assess a priori. Satellite derived gravity variations could serve as a constraint to these data, as shown for the Iquique-Pisagua earthquake, since these data present homogeneous quality and complete regional coverage (not achieved by other geodetical methods). In particular, for the Pisagua earthquake (which presented a long-term preparation phase), we had the unique opportunity to compare satellite gravity measurements from the mission GOCE with results from a dense and well-developed GPS network with more than 10 years of measurements in time and space.

Geoid height paired anomaly presented here could be explained in part from slow-slip motion and by aseismic slip, while continuous decrease along the entire marine forearc along the central segment could be the expression of subsidence in a region with higher coupling between both plates. The differences found between these three segments with different mechanical behaviour may be related to differential degree of elastic energy accumulation during the interseismic period. In back slip modelling [58], it is commonly assumed that deformation during the interseismic period constitutes a mirror image of coseismic deformation [59], which is highlighted in this work by geoid changes prior to the earthquake.

Acknowledgments

Authors acknowledge the use of the GMT-mapping software provided by Wessel, P.The authors would like to thank CONICET and Dra. Marianne Mètois for providing us the ISC model.

References

[1] E. Kendrick, M. Bevis, R. Smalley, B. Brooks, An integrated crustal velocity field for the Central Andes, Geochem. Geophys. Geosyst. 2 (2001), https://doi.org/10.1029/2001GC000191.
[2] J. Cortés-Aranda, G. González, D. Rémy, J. Martinod, Normal upper plate fault reactivation in northern Chile and the subduction earthquake cycle: from geological observations and static Coulomb Failure Stress (CFS) change, Tectonophysics 639 (2015) 118–131, https://doi.org/10.1016/j.tecto.2014.11.019.
[3] H.F. Reid, The Mechanics of the Earthquake, the California Earthquake of April 18, 1906. Report of the State Investigation Commission, vol. 2, Carnegie Institution of Washington, Washington D.C., 1910.
[4] K. Mogi, Earthquake Prediction, Academic Press Inc. EUA, 1985.
[5] E. Contreras-Reyes, J.A. Ruiz, J. Becerra, H. Kopp, C.J. Reichert, A. Maksymowicz, C. Arraigada, Structure and tectonics of the central Chilean margin (31°–33°S): implications for subduction erosion and shallow crustal seismicity, Geophys. J. Int. 203 (2) (2015) 776–791, https://doi.org/10.1093/gji/ggv309.
[6] M. Chlieh, H. Perfettini, H. Tavera, J. Avouac, D. Remy, J. Nocquet, F. Rolandone, F. Bondoux, G. Gabalda, S. Bonvalot, Interseismic coupling and seismic potential along the Central Andes subduction zone, J. Geophys. Res. 116 (2011) B12405, https://doi.org/10.1029/2010JB008166.
[7] L. Li, T. Lay, K.F. Cheung, L. Ye, Joint modeling of teleseismic and tsunami wave observations to constrain the 16 September 2015 Illapel, Chile, MW 8.3 earthquake rupture process, Geophys. Res. Lett. 43 (2016), https://doi.org/10.1002/2016GL068674.
[8] R. Bürgmann, M.G. Kogan, G.M. Steblov, G. Hilley, V.E. Levin, E. Apel, Interseismic coupling and asperity distribution along the Kamchatka subduction zone, J. Geophys. Res. 110 (2005) B07405, https://doi.org/10.1029/2005JB003648.
[9] H. Perfettini, J.P. Avouac, H. Tavera, A. Kositsky, J.M. Nocquet, F. Bondoux, M. Chlieh, A. Sladen, L. Audin, D.L. Farber, P. Soler, Seismic and aseismic slip on the Central Peru megathrust, Nature 465 (2010) 78–81, https://doi.org/10.1038/nature09062.
[10] M. Moreno, M. Rosenau, O. Oncken, 2010 Maule earthquake slip correlates with pre-seismic locking of Andean subduction zone, Nature 467 (2010) 198–202, https://doi.org/10.1038/nature09349.
[11] H. Perfettini, J.P. Avouac, Stress transfer and strain rate variations during the seismic cycle, J. Geophys. Res. 109 (2004) B06402, https://doi.org/10.1029/2003JB002917.
[12] M. Metois, A. Socquet, C. Vigny, D. Carrizo, S. Peyrat, A. Delorme, E. Maureira, M.C. Valderas-Bermejo, I. Ortega, Revisiting the North Chile seismic gap segmentation using GPS-derived interseismic coupling, Geophys. J. Int. 194 (2013) 1283–1294.
[13] S.C. Han, C.K. Shum, M. Bevis, C. Ji, C.Y. Kuo, Crustal dilatation observed by GRACE after the 2004 Sumatra-Andaman earthquake, Science 313 (2006) 658, https://doi.org/10.1126/science.1128661.
[14] L. Wang, C.K. Shum, F.J. Simons, B. Tapley, C. Dai, Coseismic and postseismic deformation of the 2011 Tohoku-Oki earthquake constrained by GRACE gravimetry, Geophys. Res. Lett. 39 (2012) L07301, https://doi.org/10.1029/2012GL051104.
[15] L. Wang, C.K. Shum, F.J. Simons, A. Tassara, K. Erkan, C. Jekeli, A. Braun, C. Kuo, H. Lee, D.N. Yuan, Coseismic slip of the 2010 Mw 8.8 Great Maule, Chile, earthquake quantified by the inversion of GRACE observations, Earth Planet. Sci. Lett. 335–336 (2012) 167–179, https://doi.org/10.1016/j.epsl.2012.04.044.
[16] M.J. Fuchs, J. Bouman, T. Broerse, P. Visser, B. Vermeersen, Observing coseismic gravity change from the Japan Tohoku-Oki 2011 earthquake with GOCE gravity gradiometry, J. Geophys. Res. Solid Earth 118 (2013) 1–10, https://doi.org/10.1002/jgrb.50381.
[17] O. Alvarez, S. Nacif, S. Spagnotto, A. Folguera, M. Gimenez, M. Chlieh, C. Braitenberg, Gradients from GOCE reveal gravity changes before Pisagua Mw = 8.2 and Iquique Mw = 7.7 large megathrust earthquakes, J. South Am. Earth Sci. 64P2 (2015) 15–29, https://doi.org/10.1016/j.jsames.2015.09.014.
[18] O. Alvarez, A. Pesce, M. Gimenez, A. Folguera, S. Soler, C. Wenjin, Analysis of the Illapel Mw = 8.3 thrust earthquake rupture zone using GOCE derived gradients, Pure Appl. Geophys. 174 (2017) 47–75, https://doi.org/10.1007/s00024-016-1376-y.

[19] S.L. Bruinsma, C. Förste, O. Abrikosov, J.C. Marty, M.H. Rio, S. Mulet, The new ESA satellite-only gravity field model via the direct approach, Geophys. Res. Lett. 40 (2013) 3607–3612.
[20] H. Hao, L. Xinga, Z. Liua, Y. Hanc, H. Li, Gravity variation in the Tibet area before the Nepal Ms 8.1 earthquake, Geod. Geodyn. 7 (2016) 425–431, https://doi.org/10.1016/j.geog.2016.07.009.
[21] N. Feldl, R. Bilham, Great Himalayan earthquakes and the Tibetan plateau, Nature 444 (2006) 165–170.
[22] Y. Zhu, W. Liang, Y. Xu, Medium-term prediction of MS 8.0 earthquake in Wenchuan, Sichuan by mobile gravity, Recent Dev. World Seismol. 7 (2008) 36–39.
[23] Kaixuan Kang, Hui Li, Shaoming Liu, Hongtao Hao, Zhengbo Zou, Long-term gravity changes in Tibet and its vicinity before the Nepal Ms 8.1 earthquake, J. Geod. Geodyn. 5 (2015) 742–746.
[24] S. Chen, M. Liu, L. Xing, W. Xu, W. Wang, Y. Zhu, Gravity increase before the 2015 Mw 7.8 Nepal earthquake, Geophys. Res. Lett. 43 (2016).
[25] W. Liang, G. Zhang, Y. Zhu, Y. Xu, S. Guo, Y. Zhao, F. Liu, L. Zhao, Gravity variations before the Menyuan Ms 6.4 earthquake, Geod. Geodyn. 7 (2016) 223–229, https://doi.org/10.1016/j.geog.2016.04.013.
[26] S.C. Han, J. Sauber, S. Luthcke, Regional gravity decrease after the 2010 Maule (Chile) earthquake indicates large-scale mass redistribution, Geophys. Res. Lett. 37 (2010) L23307.
[27] J.L. Chen, C.R. Wilson, B.D. Tapley, S. Grand, GRACE detects coseismic and postseismic deformation from the Sumatra-Andaman earthquake, Geophys. Res. Lett. 34 (2007) L13302.
[28] I. Panet, V. Mikhailov, M. Diament, F. Pollitz, G. King, O. de Viron, M. Holschneider, R. Biancale, J.M. Lemoine, Coseismic and post-seismic signatures of the Sumatra 2004 December and 2005 March earthquakes in GRACE satellite gravity, Geophys. J. Int. 171 (2007) 177–190.
[29] O. deViron, I. Panet, V. Mikhailov, M. Van Camp, M. Diament, Retrieving earthquake signature in grace gravity solutions, Geophys. J. Int. 174 (1) (2008) 14–20, https://doi.org/10.1111/j.1365-246X.2008.03807.x.
[30] A. Cazenave, J. Chen, Time-variable gravity from space and present-day mass redistribution in the Earth system, Earth Planet. Sci. Lett. 298 (2010) 263–274, https://doi.org/10.1016/j.epsl.2010.07.035.
[31] T.R. Song, M. Simons, Large trench-parallel gravity variations predict seismogenic behavior in subduction zones, Science 301 (2003) 630–633.
[32] R.E. Wells, R.J. Blakely, Y. Sugiyama, D.W. Scholl, P.A. Dinterman, Basin centered asperities in great subduction zone earthquakes: a link between slip, subsidence and subduction erosion? J. Geophys. Res. 108 (B10) (2003) 2507–2536, https://doi.org/10.1029/2002JB002072.
[33] O. Alvarez, S. Nacif, M. Gimenez, A. Folguera, A. Braitenberg, GOCE derived vertical gravity gradient delineates great earthquake rupture zones along the Chilean margin, Tectonophysics 622 (2014) 198–215, https://doi.org/10.1016/j.tecto.2014.03.011.
[34] N.K. Pavlis, S.A. Holmes, S.C. Kenyon, J.K. y Factor, The development and evaluation of the Earth Gravitational Model 2008, J. Geophys. Res. 117 (2012) B04406.
[35] M. Reguzzoni, D. Sampietro, An inverse gravimetric problem with GOCE data. International Association of Geodesy Symposia, Gravity Geoid Earth Obs. 135 (5) (2010) 451–456, https://doi.org/10.1007/978-3-642-10634-7_60. Springer-Verlag.
[36] R. Pail, S. Bruinsma, F. Migliaccio, C. Förste, H. Goiginger, W.D. Schuh, E. Höck, M. Reguzzoni, J.M. Brockmann, O. Abrikosov, M. Veicherts, T. Fecher, R. Mayrhofer, I. Krasbutter, F. Sansò, C.C. Tscherning, First GOCE gravity field models derived by three different approaches, J. Geod. 85 (2011) 819–843.
[37] S.L. Bruinsma, C. Förste, O. Abrikosov, J.M. Lemoine, J.C. Marty, S. Mulet, M.H. Rio, S. Bonvalot, ESA's satellite-only gravity field model via the direct approach based on all GOCE data, Geophys. Res. Lett. 41 (2014) 7508–7514, https://doi.org/10.1002/2014GL062045.
[38] F. Barthelmes, Definition of Functionals of the Geopotential and Their Calculation from Spherical Harmonic Models. Theory and Formulas Used by the Calculation Service of the International Centre for Global Earth Models (ICGEM). Scientific Technical Report, STR09/02, Revised edition, GFZ German Research Centre for Geosciences, Potsdam, Germany, January 2013. http://icgem.gfz-postdam.de/ICGEM.
[39] B. Hofmann-Wellenhof, H. Moritz, Physical Geodesy, second ed., Springer, Berlin, 2006, 286 pp.
[40] J. Janak, M. Sprlak, New software for gravity field modelling using spherical armonic, Geod. Cartogr. Horiz. 52 (2006) 1–8 (in Slovak).
[41] B. Schurr, G. Asch, S. Hainzl, J. Bedford, A. Hoechner, M. Palo, R. Wang, M. Moreno, M. Bartsch, Y. Zhang, O. Oncken, F. Tilmann, T. Dahm, P. Victor, S. Barrientos, J.P. Vilotte, Gradual unlocking of plate boundary controlled initiation of the 2014 Iquique earthquake, Nature 512 (2014) 299–302, https://doi.org/10.1038/nature13681.
[42] G.P. Hayes, M.W. Herman, W.D. Barnhart, K.P. Furlong, S. Riquelme, H.M. Benz, E. Bergman, S. Barrientos, P.S. Earle, P. Samsonov, Continuing megathrust earthquake potential in Chile after the 2014 Iquique earthquake, Nature 512 (2014) 295–298, https://doi.org/10.1038/nature13677.
[43] S. Ruiz, M. Metois, A. Fuenzalida, J. Ruiz, F. Leyton, R. Grandin, C. Vigny, R. Madariaga, J. Campos, Intense foreshocks and a slow slip event preceded the 2014 Iquique Mw = 8.1 earthquake, Science 345 (6201) (2014) 1165–1169, https://doi.org/10.1126/science.1256074.
[44] R. Bürgmann, Warning signs of the Iquique earthquake, Nature 512 (2014) 258–259.
[45] A. Socquet, J.P. Valdes, J. Jara, F. Cotton, A. Walpersdorf, N. Cotte, S. Specht, F. Ortega-Culaciati, D. Carrizo, E. Norabuena, An 8 month slow slip event triggers progressive nucleation of the 2014 Chile megathrust, Geophys. Res. Lett. 44 (2017) 4046–4053, https://doi.org/10.1002/2017GL073023.
[46] S.P. Nishenko, Seismic Potential for large and great interplate earthquakes along the Chilean and southern Peruvian margins of South America. A quantitative reappraisal, J. Geophys. Res. 90 (1985) 3589–3615.
[47] C. Lomnitz, Major earthquakes of Chile: a historical survey, 1535–1960, Seismol. Res. Lett. 75 (2004) 368–378.
[48] S. Cesca, F. Grigoli, S. Heimann, T. Dahm, M. Kriegerowski, M. Sobiesiak, A. Tassara, M. Olcay, The Mw 8.1 2014 Iquique, Chile, seismic sequence: a tale of foreshocks and aftershocks, Geophys. J. Int. 204 (2016) 1766–1780.
[49] R. vonHuene, D.W. Scholl, Observations at convergent margins concerning sediment subduction, subduction erosion, and the growth of continental crust, Rev. Geophys. 29 (1991) 279–316.
[50] J. Adam, C.D. Reuther, Crustal dynamics and active fault mechanics during subduction erosion. Application of frictional wedge analysis on to the North Chilean Forearc, Tectonophysics 321 (2000) 297–325.
[51] S. Lamb, P. Davis, Cenozoic climate change as a possible cause for the rise of the Andes, Nature 425 (2003) 792–797.
[52] D. Völker, M. Wiedicke, S. Ladage, C. Gaedicke, C. Reichert, K. Rauch, W. Kramer, C. Heubeck, Latitudinal variation in sedimentary processes in the Peru-Chile Trench off Central Chile, in: Oncken, et al. (Eds.), The Andes-Active Subduction Orogeny, Frontiers in Earth Science Series, Part II, Springer-Verlag, Berlin Heidelberg New York, 2006, pp. 193–216, https://doi.org/10.1007/978-3-540-48684-8_9.
[53] S. Leon-Rios, S. Ruiz, A. Maksymowicz, F. Leyton, A. Fuenzalida, R. Madariaga, Diversity of the 2014 Iquique's foreshocks and aftershocks: clues about the complex rupture process of a Mw 8.1 earthquake, J. Seismol. 20 (4) (2016) 1059–1073, https://doi.org/10.1007/s10950-016-9568-6.
[54] M. Bouchon, V. Durand, D. Marsan, H. Karabulut, J. Schmittbuhl, The long precursory phase of most large interplate earthquakes, Nat. Geosci. 6 (4) (2013), https://doi.org/10.1038/ngeo1770.
[55] D. Bassett, A.B. Watts, Gravity anomalies, crustal structure, and seismicity at subduction zones: 1. Seafloor roughness and subducting relief, Geochem. Geophys. Geosyst. 16 (2015) 1508–1540, https://doi.org/10.1002/2014GC005684.
[56] D. Bassett, A.B. Watts, Gravity anomalies, crustal structure, and seismicity at subduction zones: 2. Interrelationships between fore-arc structure and seismogenic behavior, Geochem. Geophys. Geosyst. 16 (2015) 1541–1576, https://doi.org/10.1002/2014GC005685.
[57] D.L. Kohlstedt, B. Evans, S.J. Mackwell, Strength of the lithosphere: constraints imposed by laboratory experiments, J. Geophys. Res. 100 (B9) (1995) 17,587–17,602.
[58] J.C. Savage, A dislocation model of strain accumulation and release at a subduction zone, J. Geophys. Res. 88 (1983) 4984–4996, https://doi.org/10.1029/JB088iB06p04984.
[59] S. Li, M. Moreno, J. Bedford, M. Rosenau, O. Oncken, Revisiting viscoelastic effects on interseismic deformation and locking degree: a case study of the Peru-North Chile subduction zone, J. Geophys. Res. Solid. Earth. 120 (2015), https://doi.org/10.1002/2015JB011903.

Orlando Alvarez Pontoriero, Doctor in Geophysics. Current position as Assistant Researcher at CONICET and Professor at Instituto Geofísico y Sismologico Ing. F.S. Volponi, Facultadde Ciencias Exactas Fisicas y Naturales, Universidad Nacional de San Juan. His current research is the study of great megathrust earthquakes rupture zones and its relation to Satellite Gravity. Other research interests: Geophysics, Geodynamics, Subduction zones, earthquake forecasting and prediction.